



Rapid Communication

Multi-segment earthquakes and tsunami potential of the Aleutian megathrust

Ian Shennan^{a,*}, Ronald Bruhn^b, George Plafker^c^a Science Site, Department of Geography, Durham University, Durham DH1 3LE, UK^b Department of Geology and Geophysics, University of Utah, Salt Lake City, UT 84112-0111, USA^c U.S. Geological Survey, 345 Middlefield Road MS 977, Menlo Park, CA 94025-3591, USA

ARTICLE INFO

Article history:

Received 28 July 2008

Received in revised form

22 September 2008

Accepted 24 September 2008

ABSTRACT

Large to great earthquakes and related tsunamis generated on the Aleutian megathrust produce major hazards for both the area of rupture and heavily populated coastlines around much of the Pacific Ocean. Here we use paleoseismic records preserved in coastal sediments to investigate whether segment boundaries control the largest ruptures or whether in some seismic cycles segments combine to produce earthquakes greater than any observed since instrumented records began. Virtually the entire megathrust has ruptured since AD1900, with four different segments generating earthquakes >M8.0. The largest was the M9.2 great Alaska earthquake of March 1964 that ruptured ~800 km of the eastern segment of the megathrust. The tsunami generated caused fatalities in Alaska and along the coast as far south as California. East of the 1964 zone of deformation, the Yakutat microplate experienced two >M8.0 earthquakes, separated by a week, in September 1899. For the first time, we present evidence that earthquakes ~900 and ~1500 years ago simultaneously ruptured adjacent segments of the Aleutian megathrust and the Yakutat microplate, with a combined area ~15% greater than 1964, giving an earthquake of greater magnitude and increased tsunamigenic potential.

© 2008 Elsevier Ltd. All rights reserved.

1. Context and aims

The M9.2 great Alaska earthquake of 1964 (Plafker, 1969) is one of the three largest earthquakes measured, along with Chile 1960, M9.5 and Indonesia 2004, M9.2. The 1964 earthquake initiated along the collisional contact between the Yakutat microplate and North America and then propagated westward >800 km along the eastern Aleutian megathrust, with a rupture area ~200,000 km². Onshore, the eastern limit of rupturing and coseismic uplift (Fig. 1) terminated where the sediment-filled Aleutian trench projects into a significant structural boundary within the Yakutat microplate near Cape Suckling (Bruhn et al., 2004). This boundary is >100 km west of the active deformation front defined by the Pamplona – Malaspina thrust front (Bruhn et al., 2004; Plafker, 1987), raising the possibility of greater earthquake and tsunami potential should rupturing like that in 1964 continue farther eastward within the Yakutat microplate, into the Yakataga seismic gap (Savage et al., 1986). We use the term segment for each part of the megathrust that has ruptured in large to great historic earthquakes or is the gap between rupture segments (Nishenko and Jacob, 1990); less commonly, megathrust rupture segments may also be inferred

from historic tsunamigenic events and/or paleoseismic data (Carver and Plafker, 2008). Here we use paleoseismic records to investigate whether segment boundaries control the largest ruptures (Taylor et al., 2008) or whether in some seismic cycles earthquakes greater than any observed since instrumented records began occur by rupturing through such boundaries (Nanayama et al., 2003).

2. Regional setting

The 1964 rupture produced coseismic subsidence over an elongate region including most of Cook Inlet, with uplift seaward of the subsidence zone (Fig. 1). Paleoseismic investigations around Cook Inlet record six other great earthquakes in the past 4000 years but with some differences in the spatial pattern of deformation (Shennan et al., 2008; Shennan and Hamilton, 2006). At Alaganik Slough (Fig. 1), within the 1964 zone of coseismic uplift, sediment sequences record multiple earthquake cycles (Plafker et al., 1992), demonstrating coseismic uplift and sufficient interseismic subsidence to produce net long-term subsidence. Radiocarbon ages correlate Alaganik Slough and Cook Inlet, with the last two earthquakes dated ~900 and 1500 BP (abbreviations for the 95% age ranges 910–780 cal BP and 1520–1350 cal BP) (Shennan et al., 2008).

Slip on the Aleutian megathrust explains most of the deformation, although slip on subsidiary faults caused small areas of larger vertical uplift. In one of these areas, Middleton Island (Fig. 1b),

* Corresponding author. Tel.: +44 191 3341934; fax: +44 191 3341801.

E-mail addresses: ian.shennan@durham.ac.uk (I. Shennan), ron.bruhn@utah.edu (R. Bruhn), gplafker@usgs.gov, gplafker@earthlink.net (G. Plafker).

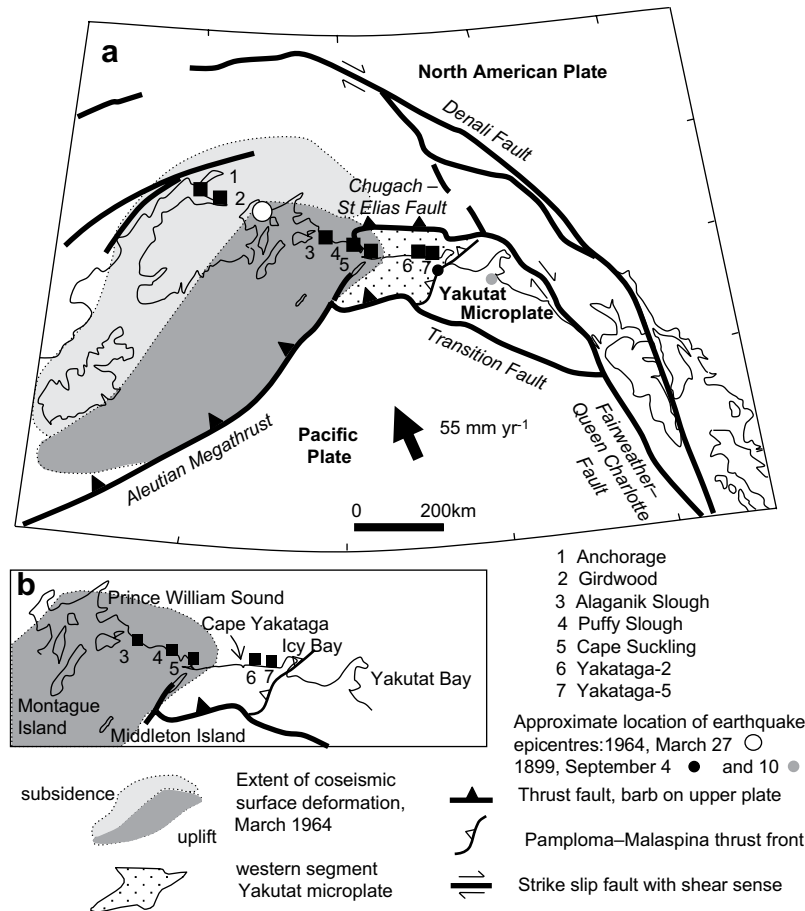


Fig. 1. (a) Tectonic setting of the eastern sector of the Aleutian megathrust and Yakutat microplate and the extent of coseismic surface deformation in the M9.2 1964 earthquake. Epicentre locations estimated by [Doser \(2006\)](#). Sites studied numbered 1 through 7. (b) Sites along the Gulf of Alaska coast.

lesser uplift in 1964 compared to previous great earthquakes may indicate a smaller area of rupture in 1964 than in previous seismic cycles, and surface faulting on Montague Island ([Fig. 1](#)) may have partly inhibited rupturing farther to the east ([Carver and McCalpin, 1996](#); [Plafker et al., 1982](#)). These interpretations pose the question – does the megathrust ever rupture farther eastward than in 1964, to the Pamplona–Malaspina thrust front?

East of the limit of deformation in 1964, raised shoreline features between Cape Yakataga and Yakutat Bay are located within the Yakataga seismic gap which last ruptured in 1899 ([Savage et al., 1986](#)) and provide evidence of episodic coseismic deformation between ~5000 BP and AD1899 ([Fig. 1](#)). Though partially buried by debris fans, paleo-cliffs between Cape Yakataga and Icy Bay indicate net uplift of ~50 m in ~5000 yr ([Plafker et al., 1982](#)). In 1899 a M8.1 earthquake near Icy Bay on September 4th produced ~1 m uplift at Cape Yakataga, but the pattern of uplift farther east is less certain ([Jacoby and Ulan, 1983](#)), and a second earthquake, September 10th M8.2, near Yakutat caused uplift ~2–14 m around Yakutat Bay ([Doser, 2006](#); [Plafker and Thatcher, 2008](#)). Neither earthquake produced a damaging tsunami ([Tarr and Martin, 1914](#)), suggesting that rupturing was mostly confined landward of the coast.

3. Evidence of vertical displacement/relative sea-level change

Here we present paleoseismological evidence from sites on either side of the eastern limit of deformation in 1964 to determine whether rupture zones of any earlier great earthquakes included the area between the limit of the 1964 rupture and Icy Bay.

3.1. Coseismic vertical displacement in 1964

Anchorage and Girdwood record coseismic subsidence and Alaganik Slough, Puffy Slough and Cape Suckling lie within the zone of uplift ([Fig. 1](#)). Uplift died out along the coast east of Cape Suckling, and did not affect the coast within the Yakataga seismic gap between Cape Yakataga and Icy Bay ([Savage et al., 1986](#)).

3.2. Coseismic vertical displacement ~900 BP

Sediment sequences beneath freshwater and tidal marshes record coseismic subsidence ~900 BP at Anchorage and Girdwood ([Hamilton and Shennan, 2005](#); [Hamilton et al., 2005](#)). Previous investigations around Prince William Sound and Alaganik Slough ([Fig. 1](#)) indicate simultaneous uplift within the 1964 uplift zone and subsequent interseismic subsidence, leading to net subsidence ([Plafker et al., 1992](#); [Plafker and Thatcher, 2008](#)). We have new cores at Alaganik Slough, Puffy Slough and immediately west of Cape Suckling ([Fig. 1](#) and [Table 1](#)). At each site we find an intertidal silt-dominated horizon overlain by peat, with a sharp boundary between. Diatom analyses confirm the intertidal origin of the silt in each case and that each peat formed at or above the elevation of highest tides. A sharp boundary at the base of an extensive peat horizon and supporting diatom evidence indicate land uplift during an earthquake, raising intertidal mudflat above the level of high tides. In contrast a gradual transition suggests a slow change in relative sea level, perhaps as a consequence of glacio-isostatic land uplift. [Fig. 2](#) shows the evidence for uplift and possible tsunami sand at Cape Suckling marsh. The boundary between silt and peat

Table 1

Radiocarbon-dated samples. Calibrated ages given as 95% probability range rounded to nearest 10 yr in the text (Reimer et al., 2004); (Ramsey, 2001). Macrofossils dated are, in all cases, *in situ* herbaceous stems or leaves.

Site and laboratory code	Stratigraphic position of sample	Radiocarbon dating method	Material dated	Radiocarbon age $\pm 1\sigma$ BP	Calibrated age, 95% probability range cal yr BP	Reference
<i>Anchorage</i>						
Beta-184317	top of peat layer	AMS	macrofossils	940 \pm 50	946–739	Hamilton et al., 2005
Beta-184315	top of peat layer	AMS	macrofossils	1070 \pm 40	1056–929	Hamilton et al., 2005
Beta-184311	top of peat layer	AMS	macrofossils	1500 \pm 40	1512–1308	Hamilton et al., 2005
Beta-184318	top of peat layer	AMS	macrofossils	1530 \pm 40	1520–1333	Hamilton et al., 2005
<i>Girdwood</i>						
Beta-45197	rooted wood at top of peat layer	conventional	macrofossils	860 \pm 60	913–677	Hamilton and Shennan, 2005
Beta-184321	top of peat layer	AMS	macrofossils	890 \pm 40	920–714	Hamilton and Shennan, 2005
Beta-45199	rooted wood at top of peat layer	conventional	macrofossils	940 \pm 60	954–731	Hamilton and Shennan, 2005
CAMS-93958	top of peat layer	AMS	macrofossils	955 \pm 40	948–764	Hamilton and Shennan, 2005
Beta-184326	top of peat layer	AMS	macrofossils	1540 \pm 40	1523–1334	Hamilton and Shennan, 2005
<i>Alaganik Slough</i>						
Beta-223760	base of peat layer	AMS	macrofossils	710 \pm 40	726–562	This paper
Beta-223761	base of peat layer	AMS	macrofossils	1610 \pm 40	1601–1403	This paper
W-6123	basal 2.5–5.0 cm of peat layer	conventional	woody peat	850 \pm 120	1047–558	Carver and Plafker, 2008
M-2874	basal 2 cm of peat layer	conventional	peat	865 \pm 45	908–691	Carver and Plafker, 2008
M-2873	basal 2 cm of peat layer	conventional	peat	895 \pm 50	925–700	Carver and Plafker, 2008
A-5937	outer part of 60 cm tree stump: add ~50–100 yr for tree age?	conventional	wood	800 \pm 50	896–663	Carver and Plafker, 2008
W-6102	basal 2.5–5.0 cm of peat layer	conventional	peat	830 \pm 120	966–555	Carver and Plafker, 2008
W-6139	basal 2 cm of irregular peat layer	conventional	peat	630 \pm 140	904–319	Carver and Plafker, 2008
W-6425	basal 2 cm of peat layer	conventional	peat	920 \pm 70	953–695	Carver and Plafker, 2008
AA-4893	basal 4 cm of peat layer	AMS	peat	1446 \pm 56	1512–1277	Carver and Plafker, 2008
W-6088	basal 2.5–5.0 cm of peat layer	conventional	peat	1500 \pm 160	1805–1064	Carver and Plafker, 2008
W-6454	basal 3 cm of peat layer	conventional	peat	1480 \pm 80	1541–1274	Carver and Plafker, 2008
W-6361	wood fragments near base of peat	conventional	peat	1540 \pm 60	1540–1313	Carver and Plafker, 2008
AA-4911	basal 4 cm of peat layer	AMS	peat	1341 \pm 48	1338–1175	Carver and Plafker, 2008
<i>Puffy Slough</i>						
Beta-239239	base of peat layer	AMS	macrofossils	840 \pm 40	900–680	This paper
<i>Cape Suckling</i>						
Beta-212212	2 cm above base of peat layer	AMS	macrofossils	880 \pm 40	915–699	This paper
Beta-212211	base of peat layer	AMS	macrofossils	970 \pm 40	955–791	This paper
Beta-212213	plant fragment in 1 cm sand below peat layer	AMS	macrofossils	920 \pm 40	923–743	This paper
<i>Yakataga-2</i>						
Beta-239243	base of peat layer	AMS	macrofossils	920 \pm 40	930–740	This paper
<i>Yakataga-5</i>						
Beta-239245	3 cm above base of peat layer	AMS	macrofossils	920 \pm 40	923–743	This paper
Beta-242795	base of peat layer	AMS	macrofossils	970 \pm 40	955–791	This paper

at 25 cm (Fig. 2) marks uplift in 1964, without any indication of a tsunami. Changes in diatom assemblages suggest more uplift in ~900 BP than in 1964. Samples from herbaceous roots within the sand and *Sphagnum* macrofossils from the base of the peat give similar radiocarbon ages, ~950–700 cal BP. These, and radiocarbon ages for the base of peat farther west at Puffy Slough (840 \pm 40 BP, 900–680 cal BP) and Alaganik Slough (710 \pm 40 BP, 730–560 cal BP) correlate with the penultimate great earthquake recorded in Cook Inlet, 910–780 cal BP (Shennan and Hamilton, 2006). We infer a short hiatus between uplift and peat growth in the core from Alaganik Slough to explain the younger age of peat at that locality.

Radiocarbon ages at other sites near Alaganik Slough support this correlation (Plafker and Thatcher, 2008).

Along >50 km of coast from Cape Yakataga to Icy Bay ongoing erosion produces outcrops of intertidal, freshwater lagoon, alluvial, aeolian and debris flow sediments. Two key outcrops, Yakataga-2 and -5, record uplift of cross-bedded beach sand and their burial by lagoon sediments (Fig. 2). We interpret Yakataga-2 as uplift of beach sand to above contemporaneous storm tide level, estimating uplift of at least 2.0 \pm 0.5 m, the minimum difference between the present storm beach and the contact. The radiocarbon sample dates the uplift 930–740 cal BP. Yakataga-5, ~3 km east, shows

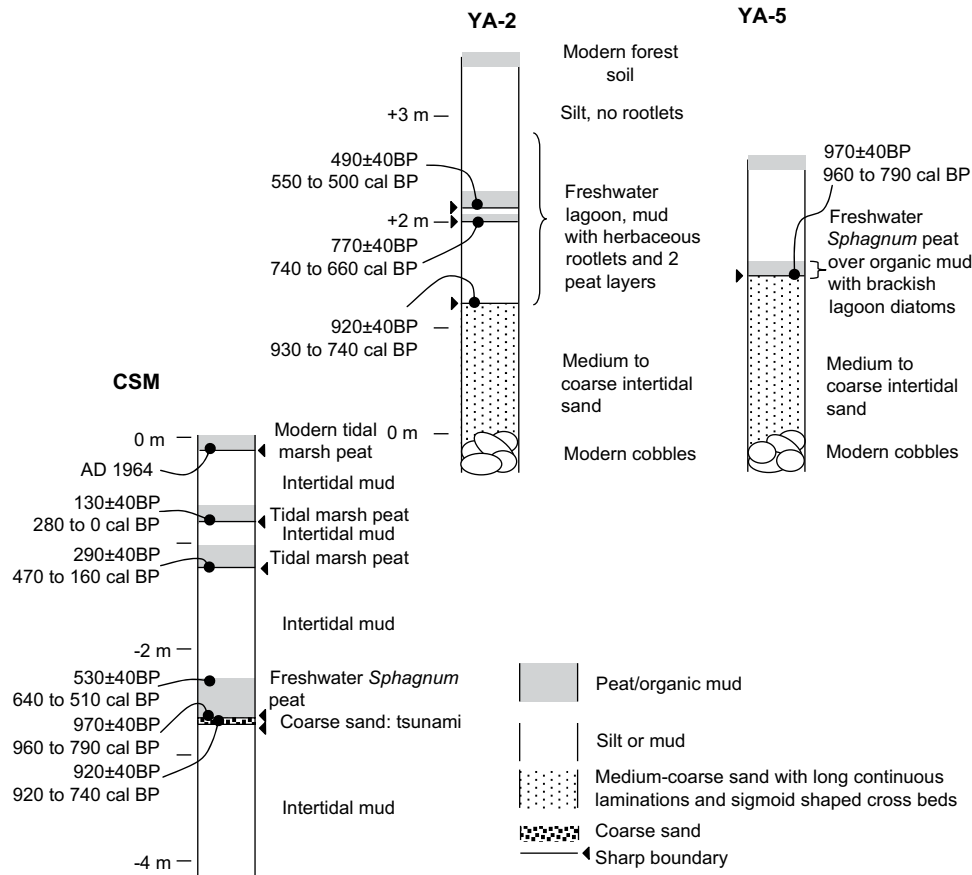


Fig. 2. Lithology, radiocarbon ages and summary interpretations of a sediment core from Cape Suckling marsh (CSM) and two exposures along the Yakataga coast (YA-2 and -5). Each drawn to same vertical scale with elevation, metres, relative to present marsh surface or storm beach cobbles. Calibrated ages are 95% probability range. At CSM, marine and brackish diatoms dominate grey laminated silt below -2.7 m. These confirm sedimentation in a tidal flat environment. A <1 cm thick coarse sand overlies the silt, with a sharp boundary between. Peat, comprising abundant *Sphagnum* moss and herbaceous roots, overlies the sand and up-core becomes silt-dominated, grading into overlying laminated silt with herbaceous roots. Diatoms show the peat dominated by freshwater and salt-intolerant diatoms which decline up-core. As silt content increases above -2.3 m, salt-intolerant diatoms decrease in abundance and marine and brackish species increase. We interpret the changes in lithology and diatoms across the base of the peat a result of rapid uplift during a great earthquake that raised the paleo-tidal flat above normal high tide level, allowing *Sphagnum* bog communities to colonise the raised surface. Coarse sand between the silt and peat units probably represents a tsunami caused by the earthquake. We see this sand in a series of cores in the marsh so it is unlikely to be an isolated channel flood or sand blow liquefaction deposit. At YA-2 the upper contact of the sand is very sharp, <2 mm, and exposed for ~ 100 m as an almost horizontal boundary. Diatoms from immediately above the contact and up-section to above the mid-section peat layers indicate freshwater lagoon sedimentation, merging to alluvium and the modern forest soil. We interpret the sequence as uplift of beach sand to above contemporaneous storm tide level, estimating uplift of at least 2.0 ± 0.5 m, the minimum difference between the present beach and the contact. YA-5, ~ 3 km east, shows synchronous uplift. The upper contact of the sand is again very sharp and laterally continuous over >100 m. Diatoms from immediately above the contact indicate a brackish lagoon, merging up-section to a freshwater *Sphagnum* peat. This indicates at least 1.5 ± 0.5 m uplift.

synchronous uplift, 960–790 cal BP. The upper contact of the sand is again very sharp and laterally continuous for more than 100 m. Diatoms from immediately above the contact indicate a brackish lagoon, merging up-section to a freshwater *Sphagnum* peat. This implies at least 1.5 ± 0.5 m uplift, the minimum difference between the elevations of the contact and present high tides.

LIDAR data for the whole Yakataga coast enable us to correlate exposures along the beach with the sequence of paleo-cliffs (Fig. 3) and radiocarbon ages for sediments that overlie associated raised shoreline deposits (Plafker et al., 1982). The paleo-cliffs indicate a region of permanent uplift rather net subsidence as occurs farther west. We infer that this reflects thrusting up a gently west-dipping fault ramp leading to the Pamplona–Malaspina thrust front (Bruhn et al., 2004).

3.3. Coseismic vertical displacement ~ 1500 BP

Sediment sequences at Girdwood, Anchorage and other sites around Cook Inlet record coseismic subsidence with a 95% age range of 1520–1350 cal BP (Shennan and Hamilton, 2006). A second peat at Alaganik Slough, ~ 4 m below present ground surface records uplift. Herbaceous stems and leaves directly above a sharp

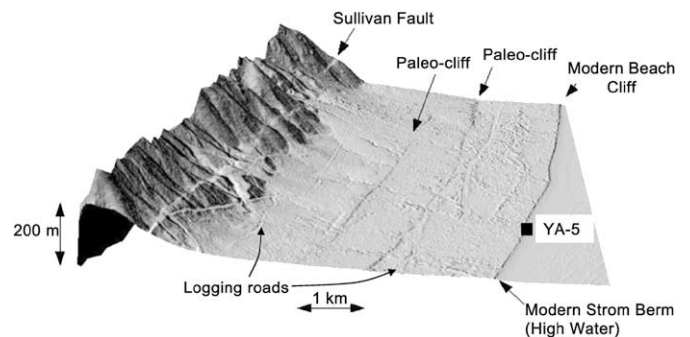


Fig. 3. LIDAR image of the Yakataga coast, sample location YA-5 at Umbrella Reef (upper Miocene facies exposed in the present intertidal zone). The image reveals the inner paleo-cliff for ~ 50 km from Cape Yakataga to Icy Bay (Fig. 1) and the more seaward paleo-cliff for at least 12 km in the region of YA-2 and YA-5. Lack of exposed sections and thick vegetation cover make further correlation less certain but the LIDAR image suggests we can trace it for a total of 20 km before it is lost to coastal erosion ~ 2 km east of YA-5. Debris fans and associated alluvial and lagoonal deposits overlie the shorelines associated with each paleo-cliff. Correlations with sediment stratigraphy and radiocarbon ages shown in Fig. 4.

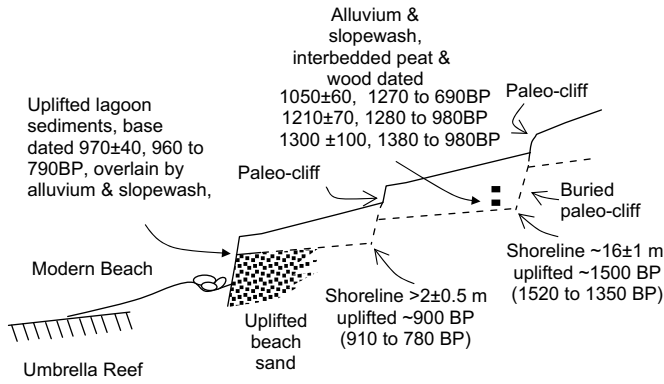


Fig. 4. Schematic summary of the coastal geomorphology and sediment stratigraphy of the Yakataga coast at Umbrella Reef, locations YA-2 and -5, correlated with paleo-cliff III, terrace fragments and associated radiocarbon ages from Plafker et al. (1982). Elevation is relative to mean higher high water. Shoreline ages based on correlations discussed in the text. The reef is erosionally truncated, steeply dipping sedimentary rock.

boundary to underlying laminated silt with intertidal diatoms, gave a radiocarbon age 1610 ± 40 BP, 1600–1400 cal BP, in agreement with other investigations from the area (Carver and Plafker, 2008; Plafker et al., 1992; Plafker and Thatcher, 2008).

Along the Yakataga coast we can trace an uplifted paleo-cliff for >50 km. It must be older than dated samples from within sediments that overlie the associated shoreline (Fig. 4) (Plafker et al., 1982). We are cautious about the precision of the ages for bulk peat samples from Yakataga because of concerns about using radiocarbon ages on bulk peat samples around Cook Inlet, where contamination by old carbon may occur (Hamilton et al., 2005). In addition to the published ages (Fig. 4) we have multiple radiocarbon ages from four other sections along the Yakataga coast. Minimum ages for uplift range from 1510 ± 40 BP, 1520–1310 cal BP, on bulk peat to 1300 ± 40 BP, 1170–1300 cal BP, on wood. Notwithstanding our caution, all of these are consistent with uplift along the Yakataga coast at the same time as uplift at Alaganik Slough and subsidence around Cook Inlet. Estimates for coseismic uplift of the paleo-cliff and associated shoreline range from ~6 m to 20 m above present (Plafker et al., 1982). With a minimum of 2.0 ± 0.5 m uplift ~900 BP this implies that the ~1500 BP uplift was ~4–18 m, approximately the same to an order of magnitude greater.

4. Discussion

We use the data from all of the sites between Cook Inlet and Icy Bay to contrast different patterns of coseismic and net deformation for three seismic cycles that generated great earthquakes (Fig. 5).

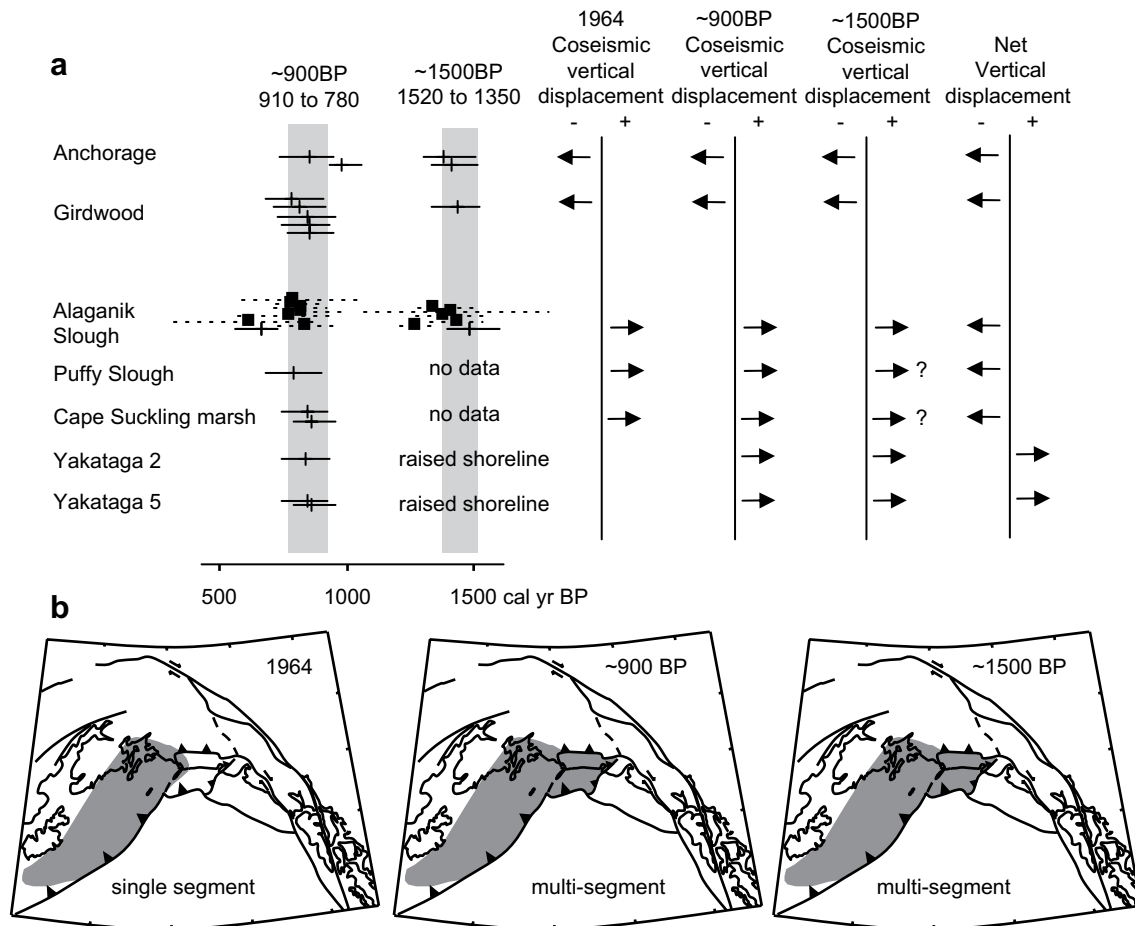


Fig. 5. (a) Coseismic and long-term net vertical displacement through three seismic cycles for a transect from Cook Inlet to Yakataga (sites 1–7, Fig. 1). Subsidence shown as negative, uplift as positive. Radiocarbon ages shown for AMS-dated samples from *in situ* herbaceous macrofossils [solid line] with additional ages from bulk peat samples [dotted line] (we acknowledge possible errors from bulk peat samples in Cook Inlet (Hamilton et al., 2005) possibly due to coal deposits within the catchment but for Alaganik Slough we identify no similar source). A hiatus may occur due to sediment erosion of the top of a peat layer as tidal flat processes impact a previous freshwater environment, in the case of site in the area of coseismic subsidence, or a delay in colonization of uplifted tidal flat by peat-forming communities in the case of a site in the area of coseismic uplift. Yakataga raised shoreline ages interpreted from data shown in Fig. 4, (b) extent of inferred coseismic uplift during great earthquakes in 1964, ~900 BP and ~1500 BP. We argue for synchronous rupturing of the segments in both ~900 BP and ~1500 BP.

Error terms for dating deposits (Table 1) mean that radiocarbon dates alone cannot provide unequivocal evidence of simultaneous rupture of segments compared to single-segment ruptures within a few decades.

This requires considering two scenarios given the structural setting and historical earthquake history of the region: 1) simultaneous rupturing of the megathrust from Cook Inlet in the west to the Pamplona – Malaspina thrust front in the east in which the Yakataga seismic gap ruptures in conjunction with the Aleutian megathrust, and 2) a rupture scenario like that of the 1899 Yakataga and 1964 earthquakes, where the Yakataga seismic gap and Aleutian megathrust ruptured independently. Two lines of evidence support the simultaneous rupture scenario for both the ~900 BP and ~1500 BP great earthquakes (Fig. 5). First, greater coseismic deformation at Cape Suckling in ~900 BP than in 1964 suggests that the area of surface deformation extended farther east. Second, the more widespread evidence for uplift east of Cape Yakataga in both ~900 BP and ~1500 BP than in 1899.

Different temporal patterns of rupturing may reflect complex stress interactions between the adjacent plate boundary faults; the Yakataga section of the megathrust links to the Chugach–Saint Elias thrust to the north which last ruptured in 1979 (M7.3), and the Fairweather transform fault and associated blind thrusts to the southeast which last ruptured in 1958 (M7.9) (Savage et al., 1986) and 1988 respectively. The earthquake history of these adjacent faults must impact loading of the Aleutian megathrust within the Yakataga seismic gap (Elliott et al., 2007; Plafker and Thatcher, 2008), apparently restricting rupturing within the landward area as in 1899, but sometimes allowing strain to accumulate and megathrust ruptures to propagate from west to east both on and offshore as we propose at ~900 and ~1500 BP. This is partly analogous to the temporal variations in rupturing proposed between the Cascadia megathrust and northern San Andreas fault (Goldfinger et al., 2008).

4.1. Implications of multi-segment earthquakes

Our new evidence for widespread rupturing within the Yakutat microplate has significant implications for the tsunami potential and seismic hazards of the Gulf of Alaska. For the ~900 and ~1500 BP earthquakes we calculate an additional 23,000 km² rupture area and ~15% increase in seismic moment compared to the 1964 M9.2 earthquake. But the increase in tsunami potential may be more significant than increased earthquake magnitude in our opinion. Rupturing as far east as the Pamplona–Malaspina thrust front involves a large area of shallow continental shelf that averages only ~0.25 km water depth, greatly increasing the likelihood of tsunami generation by coseismic uplift of the shallow sea-floor. Modelling of tsunami generation and coastline inundation for single-segment and multi-segment earthquakes at other subduction zones suggest that an increased area of sea-floor uplift during a multi-segment earthquake produces a tsunami with greater wavelength that penetrates farther inland, even though the height of the wave at the coast may be similar (Nanayama et al., 2003). In addition, the submarine escarpment of the Transition Fault (Fig. 1) forms the southern edge of the Yakutat microplate (Gulick et al., 2007; Plafker, 1987). The escarpment is over 500 km long, averages 1 km in height, and has thick Pliocene and Quaternary deposits along its top (Pavlis et al., 2004). Seismic shaking during megathrust earthquakes like those proposed ~900 BP and ~1500 BP could trigger huge submarine landslides (McAdoo and Watts, 2004) and create sea waves that propagate eastward onto the adjacent coast and southward towards more populated areas of the Pacific margin. This enhanced tsunami potential results from two fundamental geodynamic processes: 1) The submarine escarpment created by juxtaposing thicker and more buoyant lithosphere of the Yakutat microplate against less buoyant Pacific plate (Gulick et al., 2007),

and 2) vigorous erosion and accumulation of glacio-marine sediments on the continental shelf caused by rapid uplift and temperate glaciation in the Saint Elias collisional mountain belt (Gulick et al., 2004). The role of the buoyant Yakutat lithosphere is of particular interest in great earthquake and tsunami generation. Where thrust beneath southern Alaska the microplate forms a giant asperity that dominated seismic moment release and seismic slip magnitude in 1964. Farther east, the Yakutat lithosphere creates a broad and shallow continental shelf that drops off to abyssal depths where in contact with the Pacific Plate; an ideal environment for tsunami generation by landsliding if rupturing proceeds east of the 1964 earthquake limit.

5. Conclusions

Paleoseismic evidence from upper Cook Inlet and the coast of the Gulf of Alaska demonstrate coseismic deformation during great earthquakes ~900 and ~1500 years ago. The greater extent and amounts of deformation compared to those observed in AD1899 and 1964 support the hypothesis of simultaneous rupture of adjacent segments of the Aleutian megathrust and the Yakutat microplate. The alternative hypothesis is that the segments ruptured separately, during a time interval within the radiocarbon age error terms, a few decades or less. But this hypothesis less easily explains the patterns of uplift ~900 and ~1500 BP.

A multi-segment earthquake, comprising simultaneous rupture of adjacent segments of the Aleutian megathrust and the Yakutat microplate, has a combined area ~15% greater than 1964, giving an earthquake of greater magnitude and increased tsunamigenic potential.

Acknowledgements

This work is part of the NSF sponsored Saint Elias Erosion and Tectonics project (STEEP) supported by the Continental Dynamics Program, NSF 0408959 and also supported by NSF grant 9725339, NASA grant NAG-10136 and by the U.S. Geological Survey, Department of the Interior, under geologic mapping and earthquake hazards projects 1974–1993 (GP) and USGS award number 06HQGR0033 (The views and conclusions contained in this document are those of the authors and should not be interpreted as necessarily representing the official policies, either expressed or implied, of the U.S. Government).

References

- Bruhn, R.L., Pavlis, T.L., Plafker, G., Serpa, L., 2004. Deformation during terrane accretion in the Saint Elias orogen, Alaska. *Geological Society of America Bulletin* 116, 771–787.
- Carver, G.A., McCalpin, J.P., 1996. Paleoseismology of compressional tectonic environments. In: McCalpin, J.P. (Ed.), *Paleoseismology*. International Geophysics Series. Academic Press, San Diego, pp. 183–270.
- Carver, G., Plafker, G. Paleoseismicity and neotectonics of the Aleutian subduction zone – an overview. In: Freymueller, J.T., Haeussler, P.J., Wesson, R., Ekstrom, G. (Eds.), *Active Tectonics and Seismic Potential of Alaska*. In: *Geophysical Monograph Series*, vol. 179. American Geophysical Union, Washington, 350 pp., hardbound, 2008, ISBN 978-0-87590-444-3, AGU Code GM1794443.
- Doser, D., 2006. Relocations of earthquakes (1899–1917) in South-Central Alaska. *Pure and Applied Geophysics* 163, 1461–1476.
- Elliott, J., Freymueller, J.T., Larsen, C.F., 2007. Crustal deformation and strain localization in the Saint Elias Orogen, Alaska observed by GPS. *American Geophysical Union, Fall Meeting 2007*, abstract #G14A-02. American Geophysical Union, San Francisco.
- Goldfinger, C., Grijalva, K., Burgmann, R., Morey, A.E., Johnson, J.E., Nelson, C.H., Gutierrez-Pastor, J., Ericsson, A., Karabanov, E., Chaytor, J.D., Patton, J., Gracia, E., 2008. Late Holocene rupture of the Northern San Andreas fault and possible stress linkage to the Cascadia subduction zone. *Bulletin of the Seismological Society of America* 98, 861–889.
- Gulick, S., Jaeger, J., Freymueller, J., Koons, P., Pavlis, T., Powell, R., 2004. Examining tectonic-climatic interactions in Alaska and the Northeastern Pacific Eos transactions. *American Geophysical Union* 85 (433), 438–439.

- Gulick, S.P., Lowe, L.A., Pavlis, T.L., Gardner, J.V., Mayer, L.A., 2007. Geophysical insights into the transition fault debate: propagating strike slip in response to stalling Yakutat block subduction in the Gulf of Alaska. *Geology* 35, 763–766.
- Hamilton, S., Shennan, I., 2005. Late Holocene relative sea-level changes and the earthquake deformation cycle around upper Cook Inlet, Alaska. *Quaternary Science Reviews* 24, 1479–1498.
- Hamilton, S., Shennan, I., Combellick, R., Mulholland, J., Noble, C., 2005. Evidence for two great earthquakes at anchorage, Alaska and implications for multiple great earthquakes through the Holocene. *Quaternary Science Reviews* 24, 2050–2068.
- Jacoby, G.C., Ulan, L.D., 1983. Tree ring indications of uplift at Ice Cape, Alaska, related to 1899 earthquakes. *Journal of Geophysical Research* 88, 9305–9313.
- McAdoo, B.G., Watts, P., 2004. Tsunami hazard from submarine landslides on the Oregon continental slope. *Marine Geology* 203, 235–245.
- Nanayama, F., Satake, K., Furukawa, R., Shimokawa, K., Atwater, B.F., Shigeno, K., Yamaki, S., 2003. Unusually large earthquakes inferred from tsunami deposits along the Kuril trench. *Nature* 424, 660–663.
- Nishenko, S.P., Jacob, K.H., 1990. Seismic potential of the Queen Charlotte–Alaska–Aleutian seismic zone. *Journal of Geophysical Research* 95, 2511–2532.
- Pavlis, T.L., Picornell, C., Serpa, L., Bruhn, R.L., Plafker, G., 2004. Tectonic processes during oblique collision: insights from the St. Elias orogen, northern North American Cordillera. *Tectonics* 13, 1–14.
- Plafker, G., 1969. Tectonics of the March 27, 1964, Alaska earthquake. U.S. Geological Survey Professional Paper 543-I, 74.
- Plafker, G., 1987. Regional geology and petroleum potential of the northern Gulf of Alaska continental margin. In: Scholl, D.W., Grantz, A., Vedder, J.G. (Eds.), *Geology and Resource Potential of the Continental Margin of Western North America and Adjacent Ocean Basins - Beaufort Sea to Baja California*. Earth Science Series. Circum-Pacific Council for Energy and Mineral Resources, Houston, pp. 229–268.
- Plafker, G., Hudson, T., Rubin, M., Dixon, K.L., 1982. Holocene marine terraces and uplift history in the Yakutat seismic gap near Icy Cape, Alaska. U.S. Geological Survey Circular 844, 111–115.
- Plafker, G., Lajoie, K.R., Rubin, M., 1992. Determining recurrence intervals of great subduction zone earthquakes in Southern Alaska by radiocarbon dating. In: Taylor, R.E., Long, A., Kra, R.S. (Eds.), *Radiocarbon after Four Decades: An Interdisciplinary Perspective*. Springer-Verlag, New York, pp. 436–453.
- Plafker, G., Thatcher, W. Geological and geophysical evaluation of the mechanisms of the great 1899 Yakutat Bay earthquakes. In: Freymueller, J.T., Haeussler, P.J., Wesson, R., Ekstrom, G. (Eds.), *Active Tectonics and Seismic Potential of Alaska*. In: *Geophysical Monograph Series*, vol. 179. American Geophysical Union, Washington, 350 pp., hardbound, 2008, ISBN 978-0-87590-444-3, AGU Code GM1794443.
- Ramsey, C.B., 2001. Development of the radiocarbon calibration program. *Radiocarbon* 43, 355–363.
- Reimer, P.J., Baillie, M.G.L., Bard, E., Bayliss, A., Beck, J.W., Bertrand, C.J.H., Blackwell, P.G., Buck, C.E., Burr, G.S., Cutler, K.B., Damon, P.E., Edwards, R.L., Fairbanks, R.G., Friedrich, M., Guilderson, T.P., Hogg, A.G., Hughen, K.A., Kromer, B., McCormac, G., Manning, S., Ramsey, C.B., Reimer, R.W., Remmele, S., Southon, J.R., Stuiver, M., Talamo, S., Taylor, F.W., van der Plicht, J., Weyhenmeyer, C.E., 2004. IntCal04 terrestrial radiocarbon age calibration, 0–26 Cal Kyr BP. *Radiocarbon* 46, 1029–1058.
- Savage, J.C., Lisowski, M., Prescott, W.H., 1986. Strain accumulation in the Shumagin and Yakutat seismic gaps, Alaska. *Science* 231, 585–587.
- Shennan, I., Barlow, N., Combellick, R. Palaeoseismological records of multiple great earthquakes in south-central Alaska – a 4000 year record at Girdwood. In: Freymueller, J.T., Haeussler, P.J., Wesson, R., Ekstrom, G. (Eds.), *Active Tectonics and Seismic Potential of Alaska*. In: *Geophysical Monograph Series*, vol. 179. American Geophysical Union, Washington, 350 pp., hardbound, 2008, ISBN 978-0-87590-444-3, AGU Code GM1794443.
- Shennan, I., Hamilton, S., 2006. Coseismic and pre-seismic subsidence associated with great earthquakes in Alaska. *Quaternary Science Reviews* 25, 1–8.
- Tarr, R., Martin, L., 1914. *Alaskan Glacier Studies*. National Geographic Society, Washington.
- Taylor, F.W., Briggs, R.W., Frohlich, C., Brown, A., Hornbach, M., Papabatu, A.K., Meltzner, A.J., Billy, D., 2008. Rupture across arc segment and plate boundaries in the 1 April 2007 Solomons earthquake. *Nature Geosci* 1, 253–257.